ISABE-2011-1113

TIME-DOMAIN MODELING OF SCREECH-DAMPING LINERS IN COMBUSTORS AND AFTERBURNER

Guillaume Jourdain & Lars-Erik Eriksson
Chalmers University of Technology
Department of Applied Mechanics
Gothenburg, SE-41296 Sweden

Abstract

Combustor or afterburner instabilities such as buzz and screech modes can lead to major damage in gas turbines. Acoustic liners may be very effective for damping screech modes, but are also challenging to model in CFD/CAA analysis. A new time-domain porous wall sub-model is presented which enables the inclusion of acoustic liners in unsteady compressible flow solvers. The model includes linear and non-linear loss as well as inertial effects, thereby yielding the correct frequency dependent damping. Validation of the model has been carried out for standard Helmholtz type acoustic liners with zero grazing flow. Numerical studies have also been performed for an afterburner test case, with the aim of optimizing a possible screech liner. These studies include unsteady RANS computations and Arnoldi eigenmode extraction based on an LNSE solver.

Nomenclature

C_D discharge coefficient
CAA Computational Aero Acoustic
CFD Computational Fluid Dynamics
LES Large Eddy Simulation
LNSE Linearized Navier-Stokes Equations
R Linear resistance of perforate
b Length scale for oscillating air inside perforate
p pressure
k turbulent kinetic energy
u_n averaged normal velocity
u_{nss} quasi steady state value of u_n
ε turbulent dissipation
ρ density
σ wall porosity

Subscripts

1 upstream side of the perforate
2 downstream side of the perforate

Introduction

Combustors and afterburners involve a wealth of complex phenomena such as fluid dynamics, thermodynamics, acoustics, chemistry, etc. Although significant progress in the field of CFD modeling has been made in the last decade, the problem of reliable prediction of combustor instabilities remains to be solved. Two main paths may be seen when studying previous work: a) the use of unsteady RANS (URANS), Detached Eddy Simulation (DES) or Large Eddy Simulation (LES) for the direct capturing of combustion instabilities [1], and b) the use of time-domain linearized flow solvers together with an eigenmode extraction algorithm for capturing the least damped modes [2-5]. Regardless of which strategy is chosen, an important sub-modeling problem is that of combustor liners. Such liners have, in most cases, two functions: a) to protect the combustor walls from excessive heat loads, and b) to introduce acoustic damping for a selected frequency range in order to

suppress so-called combustion screech. The simplest form of liners is often seen in afterburners, consisting of a perforated plate placed some distance away from the combustor wall. By arranging a flow of coolant air between the wall and the perforated plate both surfaces are heat-protected by a combination of convection and film cooling. The acoustic damping properties are adjusted by choosing suitable values for porosity, hole size and distance between perforate and wall. For practical CFD modeling purposes the full resolution of all the geometric intricacies of a liner is not an option. Instead we must apply a model which essentially predicts the spatially averaged (or homogenized) liner response.

In this paper we present a new improved liner sub-model for time-domain flow simulations, applicable to both combustors and afterburners. The sub-model has been implemented in a state-of-the-art URANS code for compressible reactive flow and is currently being validated against detailed CFD analysis. The sub-model has also been linearized and implemented into a corresponding LNSE code. This linearized flow code is used together with an Arnoldi algorithm to extract some of the least damped eigenmodes of a combustor or afterburner. In recent work [4,5] this method was successfully applied to an afterburner test rig, the so-called Validation Rig I [6-8]. A screech mode that is known to exist at certain conditions was in fact captured, both in terms of frequency and in terms of structure. The intention in the present work is to build on this previous work by introducing various perforate plate liners in the test rig (in a modeling sense only) and evaluate how the URANS solver as well as the eigenmode extraction technique is able to capture the screech damping effects.

Methodology

The methodology, based on an existing CAA tool, is divided into three steps: 1) A reference mean solution is computed with a URANS solver based on the realizable k-ε turbulence model and an EDC-type combustion model [9]. 2) A linear flow solver based on the Linearized Navier-Stokes Equations (LNSE) is applied to compute the temporal evolution of fluctuations around the mean flow. 3) An Arnoldi eigenmode extraction procedure based on the LNSE solver is applied to compute the least damped modes of the system. This procedure provides a series of eigenvectors with corresponding frequencies and aerodynamic damping. Both linear and non-linear solvers are based on the same numerical method, the finite volume method with a 3^{rd}-order accurate upwind-biased convective flux scheme and a 2^{nd}-order compact centered diffusive flux scheme, and are run on the same block-structured non-orthogonal grid. A 3-stage Runge-Kutta scheme is chosen to perform the time stepping.

The LNSE solver is in principle built by simply linearizing, line-by-line, the URANS code. However, some changes are needed for practical reasons. For example, the turbulent kinetic energy k and the dissipation ε are excluded from the linearization process since the corresponding equations have a highly non-linear behavior. The LNSE solver uses instead the frozen eddy viscosity approach, i.e. the turbulent viscosity of the reference mean flow solution is regarded as fixed. A consequence of this choice is that the combustion model must also be excluded from the linearized solver, since it involves fluctuations of the turbulent quantities. The remaining equations in the LNSE solver are the mass transport equations (for the different species), the momen-

tum equations and the energy equation, all containing both convective and diffusive terms.

Eigenmode extraction procedure

The eigenmode extraction procedure is built on the Arnoldi algorithm combined with a time-domain linearized flow solver, in the present study the LNSE solver. The method requires, as an input, an initial perturbation field. This field should be rich in modes of oscillations which are of main interest, i.e. the least damped modes. This is easily achieved by running the linearized solver a fairly large number of time steps from a very crude initial solution.

The Arnoldi procedure builds a Krylov subspace with orthogonal eigenvectors based on the initial perturbation field. The generation of each new Krylov vector involves running the linearized solver for a given number of time steps. This means that the time step, the number of time steps and the number of Krylov vectors are initially specified before starting the procedure. When the Krylov subspace is built the Arnoldi procedure computes the eigenvectors and eigenvalues. Each eigenvector with its respective eigenvalue provides information about the structure of the oscillations for a given frequency and also the corresponding aerodynamic damping.

The Arnoldi algorithm actually extracts the least damped modes i.e. the eigenvectors which have their respective eigenvalues located in the outer part of the spectrum.

Liner sub-model

In earlier work, a model for perforated walls was derived and tested in the context of eigenmode analysis for an afterburner [3]. This model takes into account the spatially averaged flow through a porous wall according to the formula.

$$u_n = -\frac{\sigma^2 C_D^{\,2} R}{\rho_1 (1-\sigma C_D)^2} + \sigma C_D \sqrt{\frac{\sigma^2 C_D^{\,2} R^2}{\rho_1^{\,2}(1-\sigma C_D)^4} + \frac{2(p_1 - p_2)}{\rho_1 (1-\sigma C_D)^2}} \quad (1)$$

where u_n is the averaged normal velocity through the wall, σ is the porosity, C_D is the discharge coefficient for each hole, R is a laminar resistance, and the subscripts 1 and 2 refer to the upstream and downstream sides of the perforate, respectively. An additional constant was introduced to model the tangential momentum loss. Equation 1 includes both laminar viscous effects and the effects of the turbulent mixing of the individual jets formed by the holes in the perforate. However, there is one important effect missing, and that is the inertial effect. The mass of air residing in the vicinity of the holes cannot change velocity instantaneously when the pressure difference over the perforate changes rapidly; there must be an acceleration time. From simple arguments it is possible to include this inertial effect by embedding equation 1 into a simple differential equation:

$$\frac{d}{dt} u_n = \frac{(p_1 - p_2)\sigma}{b\rho_1}\left[1 - \frac{u_n}{u_{nss}}\right] \quad (2)$$

In equation 2 the parameter b is the effective 'width' of the air plug inside each hole which must be accelerated, and u_{nSS} represents the quasi steady state value of u_n according to equation 1.

From equations 1 and 2 it is now possible to study some limiting cases. First we assume that the pressure difference is so small that the laminar resistance part in equation 1 dominates. Then from equation 1 we obtain

$$u_{n_{ss}} = \frac{(p_1 - p_2)}{R} \qquad (3)$$

Inserting equation 3 into equation 2 we then obtain

$$\frac{d}{dt} u_n = \frac{(p_1 - p_2)\sigma}{b\rho_1} - \frac{R\sigma}{b\rho_1} u_n \qquad (4)$$

From equation 4 we now see that effective time scale of the inertial effect is defined by the factor $R\sigma/b\rho_1$. This is a very important parameter since it is part of what determines the resonance frequency of a liner (the other part is the distance between the perforate and the back wall).

The other limiting case is when the pressure difference is so large that we may neglect the laminar viscosity effect. Equation 1 then gives the quasi steady state

$$u_{n_{ss}} = \frac{\sigma C_D}{(1 - \sigma C_D)} \sqrt{\frac{2(p_1 - p_2)}{\rho_1}} \qquad (5)$$

Inserting equation 5 into equation 2 we then obtain

$$\frac{d}{dt} u_n = \frac{(p_1 - p_2)\sigma}{b\rho_1} - \frac{(1 - \sigma C_D)}{C_D b} \sqrt{\frac{p_1 - p_2}{2\rho_1}}\, u_n \qquad (6)$$

The factor in front of u_n is now the time scale of the inertial effect. As the pressure difference increases we see that this factor increases, implying that the dynamic response of the perforate becomes faster. This is in accordance with known facts, i.e. the inertial effects of a perforate decrease with increasing through-flow.

Validation of liner sub-model

The present extended sub-model for porous walls has been implemented in the URANS code and validated for some simple Helmholtz type acoustic liner test cases. In these test cases a porous wall with specified thickness and hole geometry was placed a certain distance from a solid back wall. Acoustic waves with normal incidence were generated and the reflected waves were computed in the CFD analysis. The computed absorption factor was then plotted for several frequencies so as to find the resonance frequency and the maximum absorption. The resulting resonance frequencies were found to be in very good agreement (within a few percent) with those given by the standard analytic expressions for Helmholtz resonators.

Further validation work for the liner sub-model is in progress, especially for non-normal incident waves and for non-zero grazing flow, but the results obtained so far were judged to be enough to claim that the present model gives the expected inertial effects that were missing in the original model.

Geometry of the Validation Rig I

The test rig is divided into two parts: an inlet part and a combustor part (Figure 1). Both parts have a width of 0.24 m and a height of 0.12 m. The inlet part is dedicated to the fuel-air mixing process. The air, initially contained in a high pressure air storage facility, enters the domain at the inlet through a choked plate whereas the fuel (propane) is released via choked multi-orifice injector tubes located 0.15 m downstream of the inlet. The fuel-air mixture passes through a combination of honeycomb and screens situated 0.122 m before the end of the inlet part, this end is 0.55 m downstream of the inlet. The combustor part has a length of 1.0 m and ends by a sudden expansion into an exhaust duct which has a cross

section 3.4 times larger than the cross section of the rig. Inside the combustor part and situated 0.682m upstream of the outlet of this part, a flame-holder is placed to stabilize the premixed flame. Its cross-section has the shape of an equilateral triangle with an edge of 4 cm.

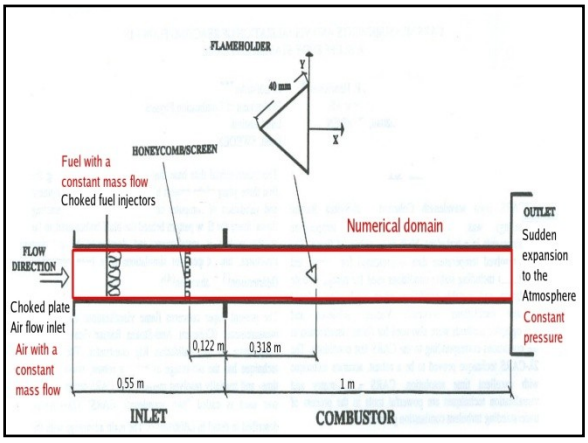

Figure 1: Geometry of the test rig and selected computational domain.

Boundary conditions

The numerical domain includes both the inlet part and the combustor part. At the inlet of the rig the choked plate ensures a constant and homogenous mass flow of air until the fuel injector tubes. The flow is also choked in the injector tubes meaning that the fuel is released with a constant mass flow through multi-orifice tubes which have equal size and which are equally distributed in the cross-section 0.15 m from the inlet of the rig. The air mass flow is fixed at the inlet boundary of the numerical domain while the fixed mass flow of fuel is generated in the numerical domain as source terms. The distance between the air inlet and the fuel injection is an important parameter since it allows fluctuations of the equivalence ratio to appear. The screens and the honeycomb located in the inlet part ensure that the fuel-air mixture entering the combustor is homogenous. They also generate three to four percent of small scale turbulence. In the CFD model the flow losses generated by the screens/honeycomb are accounted for. At the end of the rig the sudden expansion of the flow into a duct with a significantly larger cross section is modeled by a constant pressure condition.

Several experimental settings exist for the Validation Rig I, but the present study focuses on the most unstable case i.e. when two particular modes called the buzz and the screech modes are encountered in the rig (see description in next section). For this case, the mass flow, M_f, is 1.1 kg/s, the equivalence ratio, Φ, is 0.72 and the inlet temperature i.e. the temperature of the unburned mixture, T_{in}, is 288 K. The numerical domain for the test rig is extended in comparison with the experimental one to allow for the inclusion of an acoustic liner section. On each side an extra channel is added, with height 2 cm, and with only air flowing through (Figure 2). Part of the walls that separate the different gas streams are replaced by porous walls, starting 10 cm upstream of the flame-holder and ending 20 cm downstream of the rear of the flame-holder. The porous wall is investigated for three different resonance frequencies F_{pw}: 576 Hz chosen as a low frequency and 1100 Hz and 1200 Hz chosen for their closeness to the experimental frequency of the screech mode for the rig. Different values of linear resistance, R, were as well tested, ranging from 1 to 400 Ns/m3. For the studied numerical cases the only modified parameters are F_{pw}, and R.

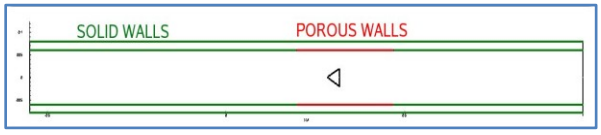

Figure 2 : Test rig with the virtual liner added.

Buzz and screech modes

Figures 3 and 4, illustrating the buzz and screech modes, were obtained from Schlieren high speed video sequences [6-8]. The buzz mode can be described as a flame flapping phenomenon with a frequency around 120 Hz. In the top left image in Figure 3, it can be observed that the large gradient in black color reveals the position of the reaction zone. On the second picture on the top right position, a variation in the length of the reaction zone leads to an increase in size of the "bubble" of burnt gases behind the flame-holder. As a result, the length of the reaction extends. This process continues until the reaction reaches the walls. At this point the length of the reaction zone is reduced and constrained by the wall and furthermore can no longer sustain a reaction rate that can maintain a pressure a sufficient level in the "bubble" of burnt gases. The pressure decreases until the "bubble" collapses on itself (bottom left picture). The reaction zone is once again large and a new "bubble" starts growing (bottom right picture).

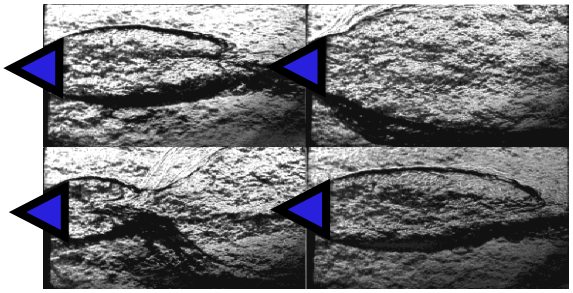

Figure 3: High speed video frames showing buzz mode in test rig (flame-holder edge 4 cm).

The screech mode has a higher frequency, 1200 Hz, and this phenomenon is characterized by "waves" in the flame front with corresponding temperature variations (Figure 4). This wave can be explained by a strong interaction between the combustion and the local vortices behind the flame-holder.

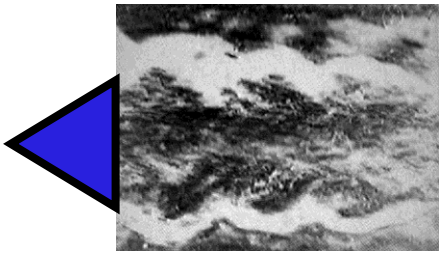

Figure 4: High speed video frame showing screech mode in test rig (flame-holder edge 4 cm).

Computational grid

The computational grid (Figures 5-6) discretizes the inlet and combustor parts of the original test rig as well as the extra "virtual" channels on the outside. These added channels are 2 cm high and have the same length as the original test rig. The overall two-dimensional domain is discretized with around 30000 cells.

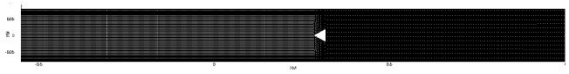

Figure 5: Computational grid.

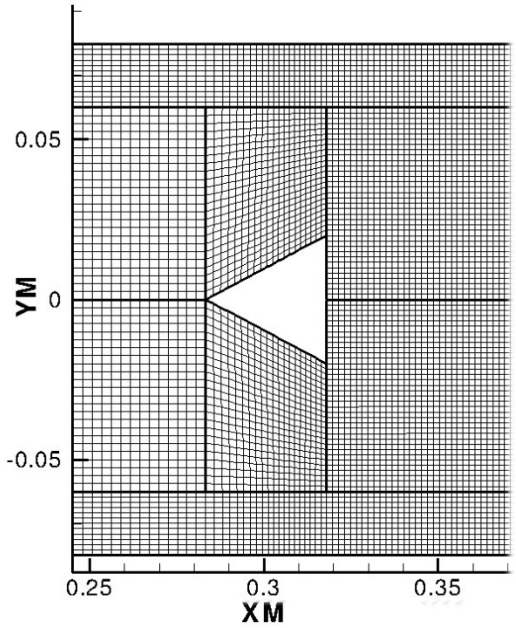

Figure 6: Enlargement of the grid in flame-holder region.

URANS solutions

In most cases the URANS solver gives unsteady solutions in which the flame front is continuously moving and deforming. If the flow solver including turbulence and combustion sub-models was good enough, the oscillations would in principle be very similar to those found in the test rig. However, our experience is that it is extremely difficult to reproduce combustion instabilities with any reliability in unsteady CFD. The main reason for this difficulty is probably the fact that existing combustion models are too simplified, so even though they give satisfactory mean flow results they do not give the correct dynamic flame response.

The presence of oscillations in URANS solutions, albeit with incorrect amplitudes, is both a nuisance and a bonus. In order to have a usable reference solution for the LNSE solver and eigenmode extraction procedure, time-averaging must be applied, which means that more time must be spent on this phase. However, the existence of oscillations also means that typical eigenmodes should be excited to some degree in the URANS solutions. This fact may be utilized by sampling for example pressure in selected points and computing the corresponding spectra. It is then possible to identify various modes and study how their amplitudes are affected by the introduction of acoustic liners.

Figure 7 shows the time-averaged solution for the following settings: the mass flow is 1.1 kg/s, Φ is 0.72, and T_{in} is 288 K. The included acoustic liner is designed to have a resonance frequency of 1200 Hz and a linear resistance of 10 Ns/m3. It had virtually no influence on the mean flow, but as will be shown in the results below it had a profound effect on the unsteady flow and flame movement. Comparisons between computed and measured mean velocity and temperature fields were performed in previous work [4,5] and were found to be satisfactory. This means also that the spreading rate of the flame brush is quite close to that found in the test rig for the same conditions.

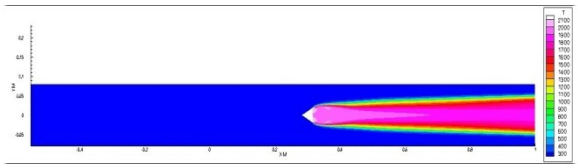

Figure 7: Averaged URANS solution showing temperature contours.

Fourier spectra and eigenmode extraction technique applied to test rig

A monitor point located at the same x-position as the beginning of the porous wall (10 cm upstream the flame holder) but close to the centerline for the y-position was used to record the fluctuations of the pressure and the velocities. Starting from a URANS solution that had reached a stationary fluctuation pattern, the solver was run for an additional 50000 time steps to record the pressure and velocity fluctuations over several periods of the slowest fluctuations. Fast Fourier transforms provided then the Fourier spectra needed to study the influence of the porous wall, Figures 8-13.

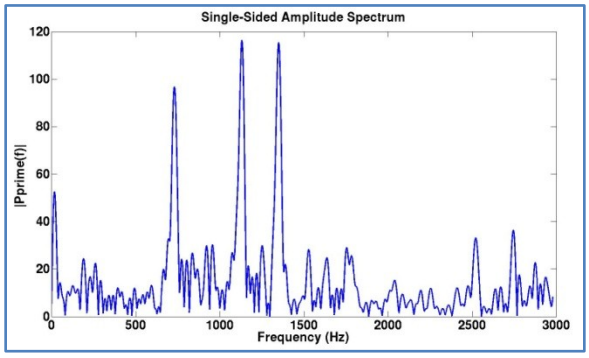

Figure 8: Case with solid walls, power spectrum of pressure

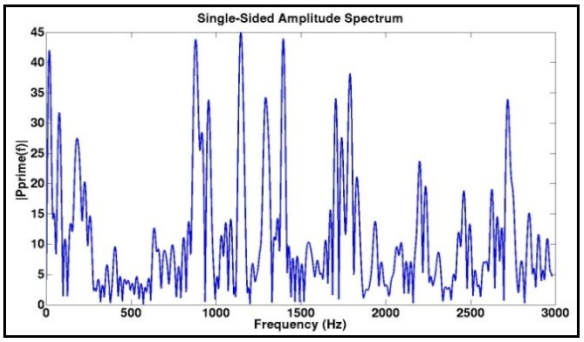

Figure 9: Case with F_{pw} = 567 Hz and R = 10, power spectrum of pressure

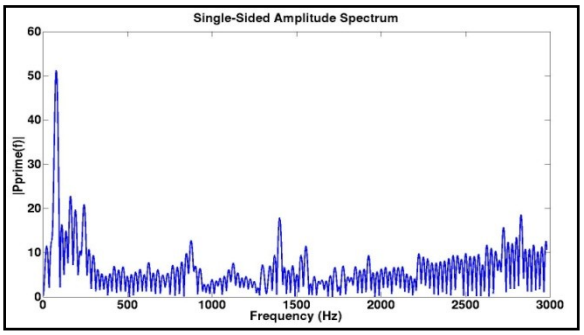

Figure 10: Case with F_{pw} = 567 Hz and R = 400, power spectrum of pressure

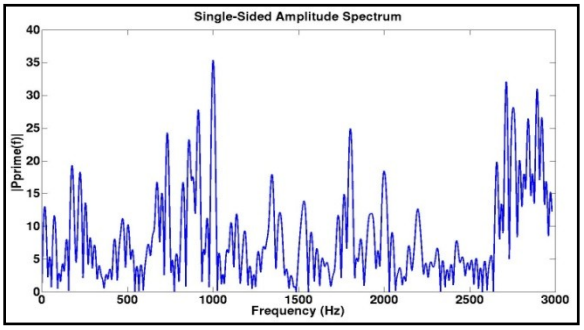

Figure 11: Case with F_{pw} = 1100 Hz, R = 10, power spectrum of pressure

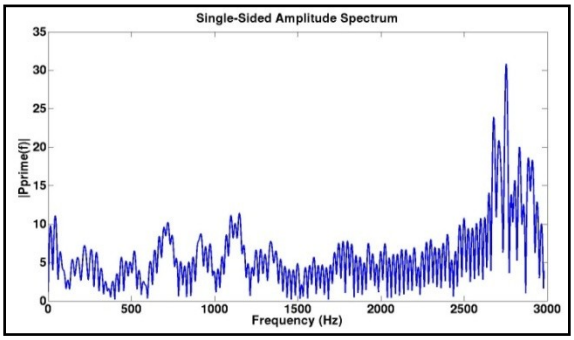

Figure 12: Case with F_{pw} = 1200 Hz, R = 10, power spectrum of pressure

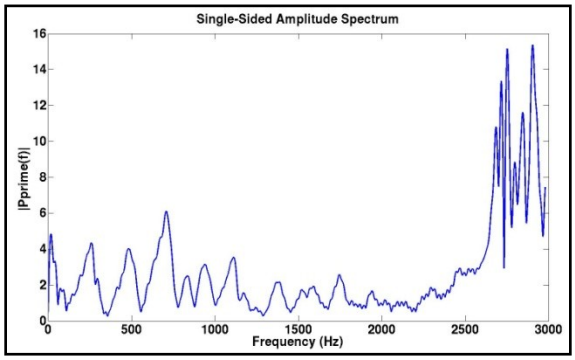

Figure 13: Case with F_{pw} = 1200 Hz, R = 400, power spectrum of pressure

Figure 8 is considered as the reference case since there are only solid walls. The power spectrum reveals several large amplitude specially for frequencies of the buzz mode (~80 Hz) and screech mode (~1150 Hz) candidates. Figures 9 and 10 present the power spectra of pressure fluctuations, for F_{pw}=567 Hz and two different linear resistances, R=10 and R=400. When R=10, the amplitudes for frequencies between 300 and 600 Hz are low meaning that the porous wall damps fluctuations with frequencies close to the resonance frequency. This shows the liner sub-model can be tuned to damp a given range of frequencies. The case R=400, which is unrealistic but still of interest as a reference case, the linear losses are more important and the Fourier spectrum reveals that the range of frequencies where the fluctuations are influenced and damped by porous wall extends to higher frequencies. For both cases the fluctuations in the frequency range of the buzz candidate, 80 Hz, remain with high amplitudes in the spectra. The candidate for the screech mode has a frequency of 1150 Hz and the amplitude of such fluctuations in pressure are damped for a linear resistance of 400, by comparing cases for the Figure 10 and 9.

In Figure 11, the linear resistance is set to 10 and the resonance frequency is now raised

to 1100 Hz. In that case, the amplitude for fluctuations with frequency of 80 Hz is still high but the amplitude for the fluctuations around the screech mode candidate frequency is low. However a new high amplitude peak with a frequency around 1000 Hz is found in the spectrum. A possible explanation is that the liner has influenced the frequency of the screech mode.

When the resonance frequency is set to 1200 Hz for the liner section, i.e. the experimental frequency of the screech mode for the test rig, the amplitude for fluctuations around the screech frequency, see Figures 12 and 13, are dramatically reduced. For the linear resistance of 10, these amplitudes are divided by twelve in comparison with their corresponding level in the Figure 8 (solid walls). It should be mentioned that very similar results were obtained for R=1, which indicates that for such small values of linear loss the non-linear loss mechanism in the porous wall model is dominating.

It may also be observed that for frequencies above 2700 Hz, the amplitudes of fluctuations are large in Figure 11, 12, 13. These fluctuations are both transversal and longitudinal modes and are not significantly damped in the studied cases.

These results show that by tuning the resonance frequency of the liner sub-model some modes of oscillations can be significantly damped, even a potentially dangerous mode such as the screech mode.

In previous work [4,5] the Arnoldi eigenmode extraction technique was applied to the same test rig, Validation Rig I. It was then possible to capture both a low frequency (~120 Hz) buzz mode and a medium frequency (~1200 Hz) screech mode. In the present work the same technique was applied to the extended computational domain that includes the liner section.

For the case with only solid walls and the cases where resonance frequency of the porous walls is 567 Hz, the buzz and the screech modes are extracted. This means that there is no significant influence of the liner on the damping. Meantime for the cases where the resonance frequency is set to 1100 Hz or 1200 Hz, the Arnoldi extraction method provided a candidate for the buzz mode (Figures 14 and 15) but none for the screech mode. This indicates that the corresponding eigenvalue of the candidate screech mode has been too damped to be extracted. The modeled liner section has thus significantly influenced the dynamics of this mode. This is in agreement with the pressure power spectra of the URANS solutions, where these cases showed a large damping effect on the screech mode.

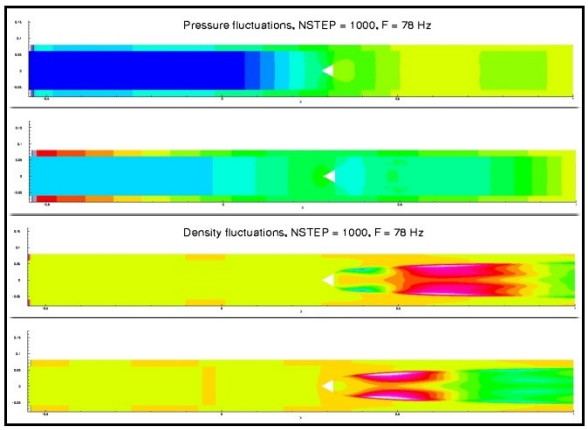

Figure 14: Buzz mode candidate for the case with F_{pw} = 1200 Hz, R = 10 (Pressure and density fluctuations, Real and imaginary parts)

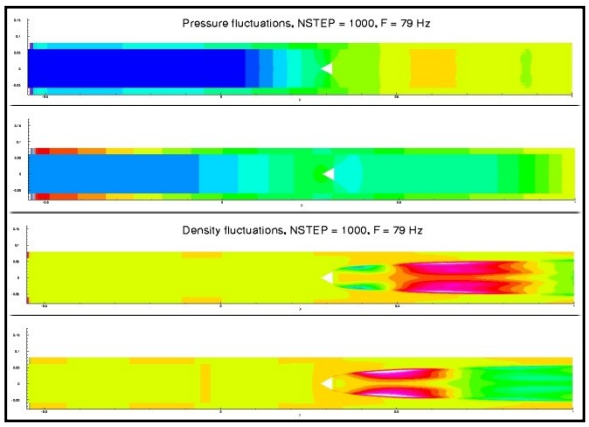

Figure 15: Buzz mode candidate for the case with F_{pw} = 1100 Hz, R = 10 (Pressure and density fluctuations, Real and imaginary parts)

Conclusions

In order to study via CFD/CAA the damping of combustion instabilities inside combustion chambers, a new liner sub-model has been investigated. The test case chosen for such investigation was the Validation Rig I where "virtual" liner sections with porous walls were included around the region of the flame-holder. The liner sub-model has been applied for different resonance frequencies, low frequency (~570 Hz) or close to the screech mode frequency (~1200 Hz), and for different linear resistances. Pressure power spectra reveal that the liner sub-model introduces sufficient damping to significantly reduce the amplitude of pressure fluctuations around a chosen frequency, in particular the fluctuations which have a frequency close to the screech mode frequency. It also appears in the spectra that an increase of the linear resistance increases the range of frequencies influenced by the liner. For the studied cases, the amplitudes of frequencies around the buzz mode frequency are not significantly damped since these frequencies are out of the range of frequencies influenced of the liner. The Arnoldi extraction technique provides also in each case a candidate for the buzz mode, but not for the screech mode. As expected, when the screech mode is significantly damped it no longer appears amongst the "least damped eigenmodes" and is therefore not captured by the Arnoldi method.

Acknowledgments

The research has been funded by the Swedish Energy Agency, Siemens Industrial Turbomachinery AB and Volvo Aero Corporation through the Swedish research program TURBO-POWER, the support of which is gratefully acknowledged. This work has been performed at the Department of Applied Mechanics, Division of Fluid Dynamics at Chalmers University of Technology.

References

1. Huang, Y., and Yang, V., "Dynamics and stability of lean-premixed swirl-stabilized combustion", Progress in Energy and Combustion Science, 35 (2009), pp. 293-364.
2. Eriksson, L.-E., Andersson, L., Lindblad, K., Andersson, N., "Development of a Cooled Radial Flame-holder for the F404/RM12 Afterburner: Part III Afterburner Rumble Prediction and Suppression", paper ISABE-2003-1060, presented at the *16th ISABE Conf*, Cleveland Ohio, September 2003.
3. Eriksson, L.-E., Moradnia, P., "Computational Study of Mixed Hydrodynamic-Acoustic Waves in Gas Turbine Afterburner Flows", paper AIAA-2950, proc. of 14th AIAA/CEAS Aero-acoustics Conf, 5-7 May 2008, Vancouver, Canada.
4. Jourdain, G. Eriksson, L.-E. ''Analysis of thermo-acoustic properties of combustors and Afterburners'', GT2010-22339,

ASME Turbo Expo 2010, June 14-18, 2010, Glasgow, UK.
5. Jourdain, G. Eriksson, L.-E. ''Combustor stability analysis based on linearized flow solvers and Arnoldi-based eigenmode extraction techniques", AIAA-2010-3866, 16th AIAA/CEAS aero-acoustics conference 2010, June 7-9, 2010, Stockholm, Sweden.
6. Sjunnesson, A., Olovsson, A. ,Sjöblom, B., "Validation Rig – A tool for flame studies", presented at 10th ISABE Conf., Nottingham, UK, September 1-6, 1991.
7. Sjunnesson, A., Nelsson, C., Max, E., "LDA measurements of velocities and turbulence in a bluff body stabilized flame", Proc. of 4th International Conf. on Laser Anemometry – Advances and Applications, ASME; Cleveland, August 1991.
8. Sjunnesson, A., Henrikson, P., "CARS measurements and visualizations of reacting flows in a bluff body stabilized flame", AIAA-92-3650, presented at 28th Joint Propulsion Conference and Exhibit, Nashville, Tennessee, July 6-8, 1992.
9. Magnussen, B. F. and B. H. Hjertager, 1976: On mathematical modeling of turbulent combustion with special emphasis on soot formation and combustion. *Sixteenth Symposium (International) on Combustion*, Pittsburgh, Pa : Combustion Institute, Cambridge,MA, USA, 719–729.